Ultramicroscopy 3 (1978) 283–290


# RECONSTRUCTION OF GLUTAMINE SYNTHETASE USING COMPUTER AVERAGING

J. FRANK and W. GOLDFARB
*Division of Laboratories and Research, New York State Department of Health, Albany, NY 12201, USA*

D. EISENBERG and T.S. BAKER *
*Molecular Biology Institute, University of California-Los Angeles. Los Angeles, CA 90024, USA*

Received 26 June 1978

The axial projection of the glutamine synthetase molecule has been reconstructed from electron micrographs of a stained preparation by using a new method of correlation search and averaging. The average over 50 individual molecules appears as a radial pattern with sixfold symmetry. The handedness evident in the average is attributed to nonuniformity of the negative stain.

## 1. Introduction

In recent years new techniques for interpreting computer images have been introduced into structural research with the electron microscope. One such technique is image averaging, now widely used to suppress substrate noise [1] and increasingly considered as a means of retrieving high resolution information from low-exposure micrographs of radiation-sensitive specimens [2]. This coherent filtering approach relies on the fact that in crystalline arrangements the repeated units are separated by integer combinations of the same basic translation vectors and that they have an identical orientation.

A large number of biological molecules, however, do not form crystals but exist as individual particles. For such specimens we are making use of a new method of averaging which does not require that the object be regularly arranged. This method employs a computer to search out the relative translation vector and orientation angle of each particle with respect to an arbitrary reference particle. We make use of correlation functions, the tool of classical approaches to pattern recognition, where only rigid body movement of the patterns is allowed.

According to electron microscopic studies by Valentine et al. [3] of glutamine synthetase (GS; EC 6.3.1.2), each molecule contains 12 subunits arranged in two eclipsed hexamers and has twofold axes perpendicular to its axis of sixfold symmetry. The maximum diameter of the hexamer face is 140 Å. Frey et al. [4] investigated seven-stranded cables formed by GS molecules under certain ionic conditions. A low-resolution three-dimensional reconstruction of these cables confirmed Valentine et al.'s data and characterized the subunits as oblate ellipsoids of revolution around axes parallel to the helical axis, with diameters of 63 Å when viewed down these axes. Arguments for the dihedral symmetry of the molecules were given by Kabsch et al. [5].

## 2. Electron microscopy

A sample of GS from *Bacillus caldolyticus* (0.1–0.5 mg/ml) was applied by the adhesion method to a carbon-stabilized, parloidion-covered electron microscope grid for 30 s, washed with 2–3 drops of double-distilled $H_2O$, stained with 2–3 drops of 1% uranyl acetate, blotted dry with filter paper, and allowed to air-dry. Electron microscopy was done without pre-

* Present address: MRC Laboratory of Molecular Biology University Postgraduate Medical School, Hills Road, Cambridge, CB22QH, England.

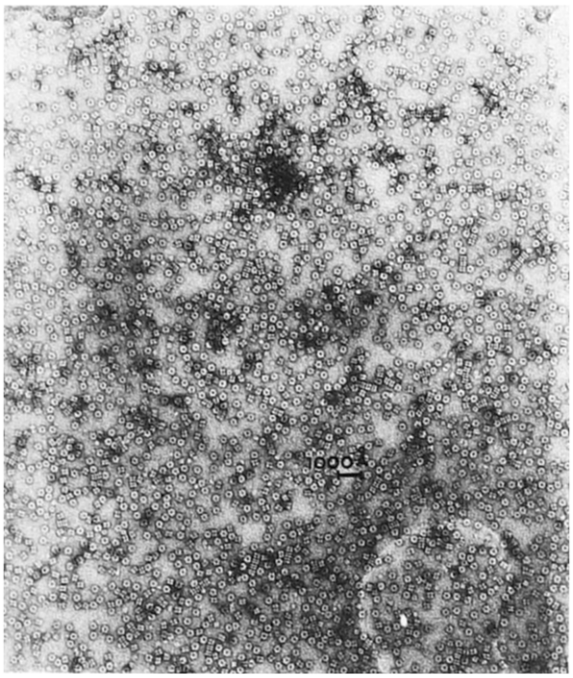

Fig. 1. Electron micrograph of glutamine synthetase from Bacillus caldolyticus stained with uranyl acetate.

cautions to limit radiation damage, using a Siemens 1 Å electron microscope at 80 kV and a nominal magnification of 46,000X. Particle size measurement determined the magnification value as 51 000X (see section 5). Optical diffraction showed a continuous transfer interval out to 0.05 $Å^{-1}$, which is sufficient to resolve the finest details to be expected in a highly irradiated, stained object. No attempt was made, therefore, to correct for instrument aberrations.

The electron micrograph (fig. 1) typically shows a large number of particles with apparent hexagonal symmetry, some lying on their side presenting a side view of the two hexamers, others stacked in long cylinders.

## 3. Image averaging

### *3.1. Principle*

Particles visible in an electron micrograph contain noise from four different sources: (i) the random structure of the carbon support film, (ii) structural variations among the particles due to preparation artifacts and beam damage, (iii) granularity of the stain, and (iv) photographic noise.

Provided these noise components are random and not correlated to the observed structure, they can be virtually eliminated by averaging over a large number of repeats of the particle. The principle of this

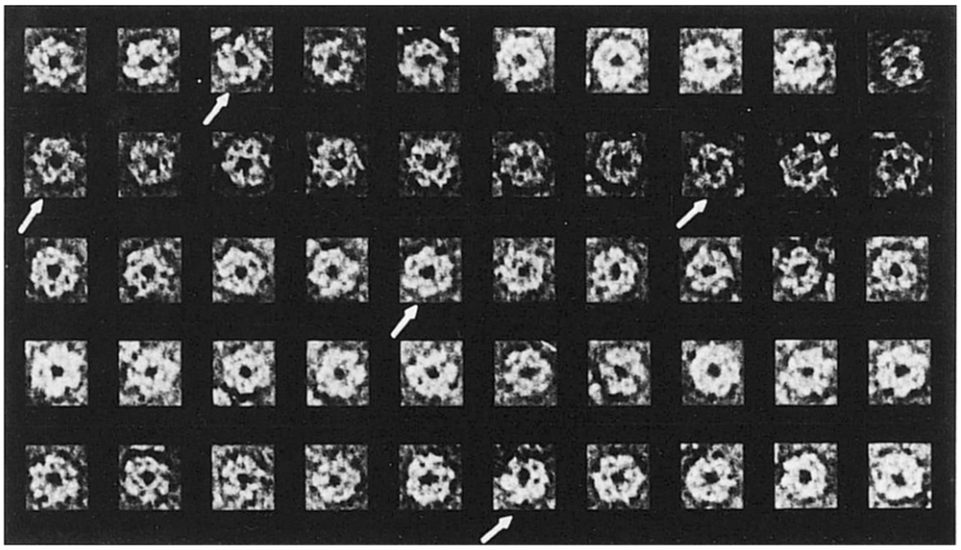

Fig. 2. Gallery of selected particles. The sidelength of the image arrays is 200 Å. Particles marked with arrows show the "windmill" features of the reconstruction (see section 4).

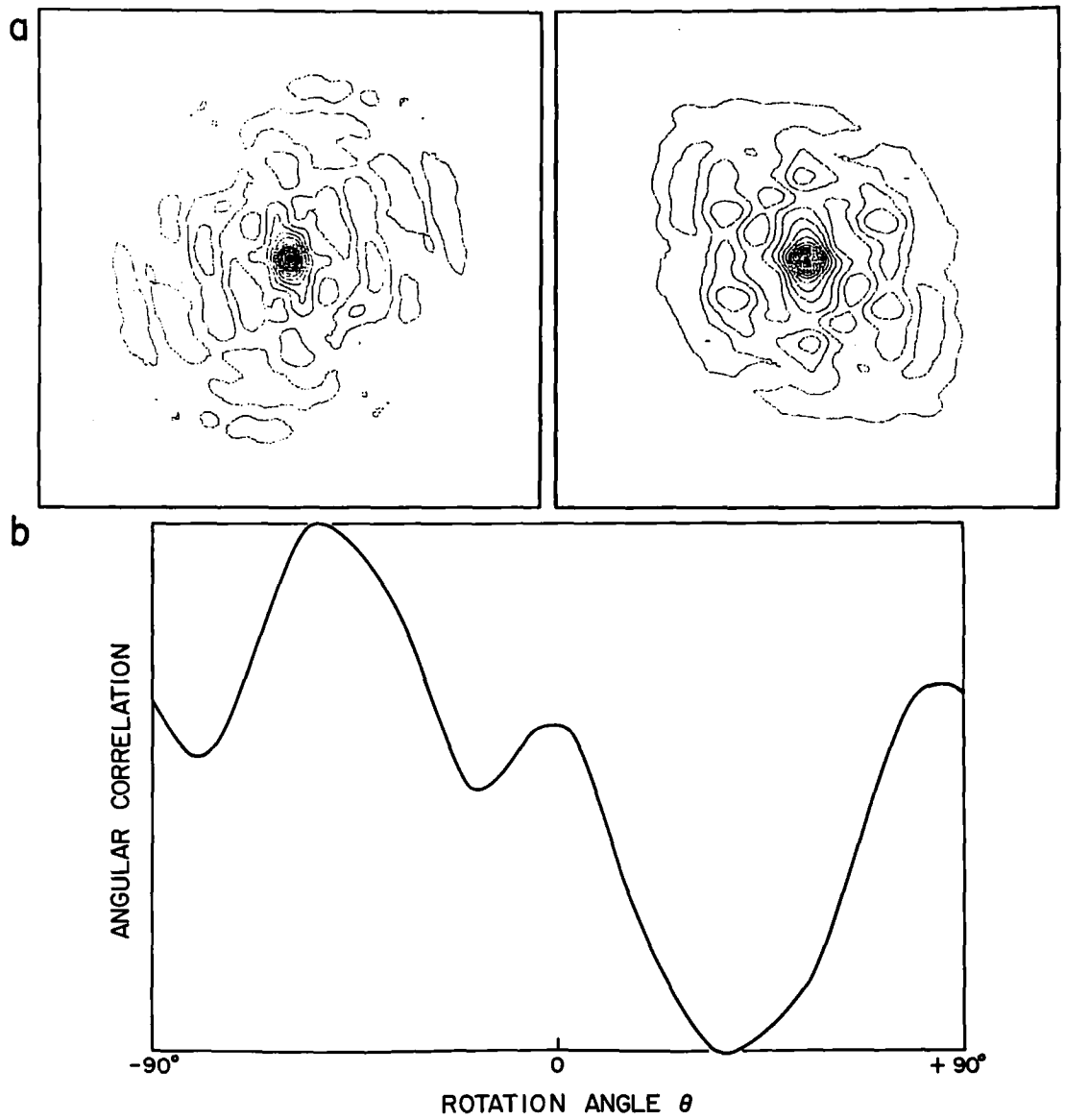


Fig. 3. Computer plots of (a) two-dimensional autocorrelation functions of two particles and (b) their averaged product (angular cross-correlation) in different relative orientations $\theta$. The three peaks within a 180° range indicate hexagonal symmetry. The computer searches the position of the maximum peak and uses the corresponding angle to rotate one of the particles into the same orientation as its reference particle.

approach is the same as that used in photographic averaging [3,6] and in averaging by computer filtration of electron micrographs of stained (e.g. [1]) and unstained [2] crystalline objects. In the latter case, averaging was used to reduce the specimen dose to a level (0.5–1.0 e/Å$^2$) where no appreciable damage occurs.

Frank's extension of the averaging method to micrographs of nonperiodic specimens with a preferential attachment to the supporting film has been outlined previously [7,8]. Computer search techniques were proposed to determine translation and orientation in the plane of attachment. A computer study [9] explored the performance of the translation

search under low-dose conditions, which is the ultimate goal of the present work. Early results of averaging studies using low-dose techniques have recently been presented [10,20].

Our approach is similar to that of Ottensmeyer et al. [11] except that (i) visual alignment is replaced by computer methods to establish the relative translation and orientation parameters and (ii) montage and optical filtration are replaced by a simple summation in the computer. We believe that for noisy images, computer alignment is crucial to assure reliable, artifact-free reconstruction.

### 3.2. Computer methods

Each reconstruction was done with 50 particles. Small areas large enough to include a GS molecule were scanned with a Perkin Elmer PDS 1010A flatbed microdensitometer. A sampling distance of 16 $\mu$m was used, corresponding to 3.14 Å at 51 000X magnification (see section 5). The particles contained in 64-by-64 image arrays (fig. 2) were brought into exact register with a reference particle by computer procedures that locate the rotation angle between two arbitrarily oriented and positioned two-dimensional motifs [12,13] and the translation vector between two motifs which have the same orientation but different translations [12–14].

For the orientation search the computer calculates the two-dimensional autocorrelation functions of the image arrays. (fig. 3a) and determines the angle at which their cross-product is maximized (fig. 3b). The size of the cross-product at the matching angle is a measure of the similarity of the autocorrelation functions or of the reproducibility of intramolecular vectors as they appear in projection. Autocorrelation functions are used because they make the orientation search independent from the translation search. A similar approach is employed in the so-called molecule-fitting methods in $x$-ray crystallography.

After the particles have been brought into matching orientation, using the angles found in the orientation search, the translation search is performed. Two image arrays will contain the same motif at different positions $r_1$ and $r_1 + \Delta r$. The two-dimensional cross-correlation function of these arrays will contain the autocorrelation function of the motif in the off-origin position $\Delta r$ and will thus show the direction and size

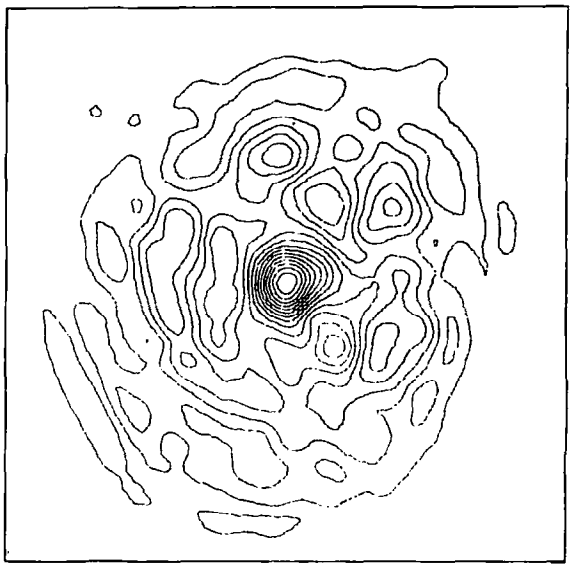

Fig. 4. Two-dimensional cross-correlation function of two GS particles that have been brought into matching orientations. The position of the peak with respect to the center indicates the relative shift between the two particles (from [19], courtesy of Springer-Verlag, Heidelberg).

of the relative translation vector (fig. 4). The size of the cross-correlation peak, when suitably normalized, is a measure of the similarity of the particles or of the reproducibility of their structure as shown in projection.

All computations were done on a PDP 11/45 under the RSX 11D executive. The software was the newly developed image-processing system SPIDER [15] in which 60 (and potentially more) operations, such as Fourier transformation, cross-correlation, rotation, and specific contrast-enhancement algorithms, can be specified in a simple command language. Through a DO loop command, any set of operations can be applied to a whole sequence of image files. The entire reconstruction – from locating the randomly positioned particles to visualizing the six-fold, rotationally averaged result – can thus be performed in a single step requiring no interaction by the user.

## 4. Results

Our approach is based on the assumption that the stained GS particles are short cylinders lying flat on

the supporting film so that an axial projection is visible at zero tilting angle, provided the warping of the film is negligible.

For any mass-density distribution within the cylinder, there are two possible axial projections, and they are mirror images of each other. An electron micrograph of an assembly of such cylinders will show two different motifs related by mirror symmetry. Only one motif will be visible if the axial projection is centrosymmetric and thus identical to its mirror image, or if the axial projection is noncentrosymmetric but the cylinder always faces the supporting grid with the same side.

Earlier studies on the structure of GS from Escherichia coli [3–5], as well as the appearance of the particles in the electron micrographs, suggest that only one motif is present. There is no clustering of the values for angular correlation or for the normalized translational cross-correlation of the particles with respect to the selected reference particle. If two noncentrosymmetric motifs related by mirror symmetry were present, two distinct clusters would be expected in the latter values: a cluster at high correlation values indicating particles facing the same way as the reference particle, and a cluster at low correlation values indicating particles facing the opposite way.

The average obtained from 50 particles (fig. 2) after alignment (figs. 5a,b) does not exhibit the expected centrosymmetry. Instead, a "windmill" pattern with cyclic symmetry is visible, with six elliptic low-density regions at the periphery of the spiral arms. This pattern is not an accidental result for the

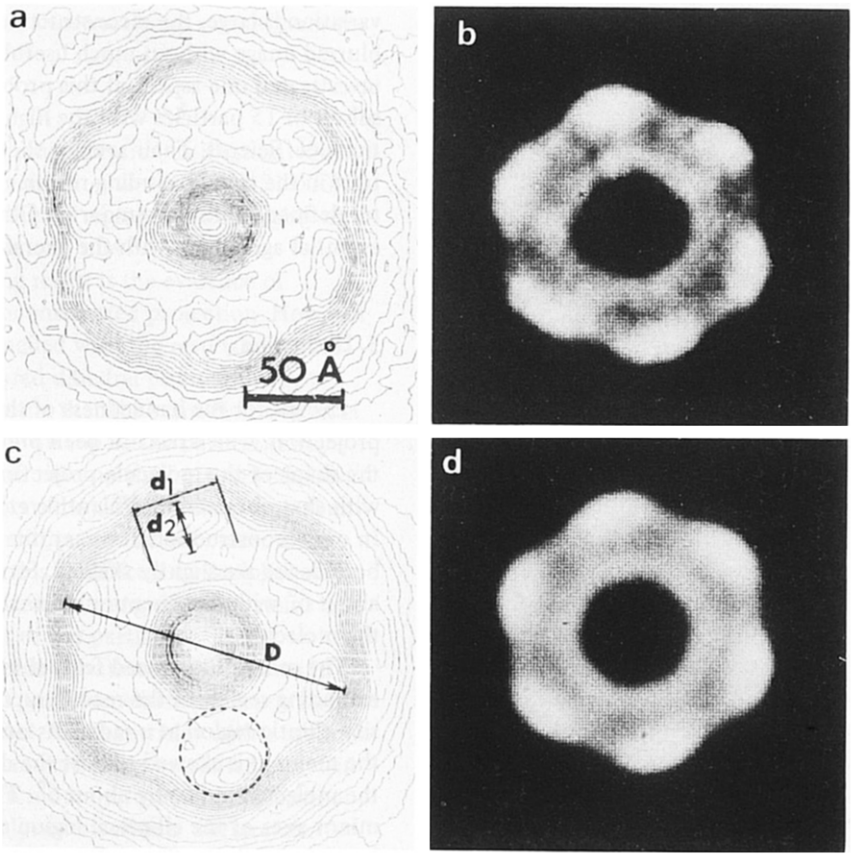


Fig. 5. Average of 50 particles: (a) contour representation; (b) enhanced gray-level display of stain-excluding region; (c) sixfold, rotationally averaged reconstruction in contour representation; and (d) same as c, with enhanced gray-level display of stain-excluding region. $D$, largest diameter scaled to 140 A; $d_1$, $d_2$, minor and major axes of the elliptic region. The dotted line marks the approximately circular subunit region.

particular set of particles chosen, as could be shown by averaging over arbitrary subsets of the particles or by averaging over a different set of 50 particles. On closer inspection, handedness is clearly visible in a number of particles (fig. 2, arrows). The result of rotational averaging using the sixfold cyclic symmetry is shown in fig. 5c,d. The subunit of the rotationally averaged particle is thus the average of 300 individual subunits, with a 17-fold-enhanced signal-to-noise ratio.

To center the averaged particle for rotational averaging, we made use of the molecules' centro-symmetry. In this procedure the image containing a centrosymmetric motif is rotated 180°, and the cross-correlation function of original and rotated images is computed. The peak indicates the relative displacement between the motif in the original image and its 180°-rotated counterpart, which would be identical in the absence of noise. A shift of the image by half of this displacement vector then brings the motif into the center of the image.

To reduce the subjective element introduced by the selection of an arbitrary reference particle, we used the average of the first run as reference for a refinement run of the reconstruction. However, the contours of the stain-excluding region did not change significantly. This indicates that the reference particle was representative of a large subset of the particles.

Another concern is the extent of structural variation within the set used for reconstruction. If this variation is large, the reconstruction will produce a blurred image without much useful information. We investigated one aspect of this problem by selecting a subset of 15 particles with the highest cross-correlation coefficients. Their average showed enhanced contrast in the stain-excluding region and somewhat better-defined subunit boundaries. Otherwise it was in essential agreement with the overall average. (fig. 6).

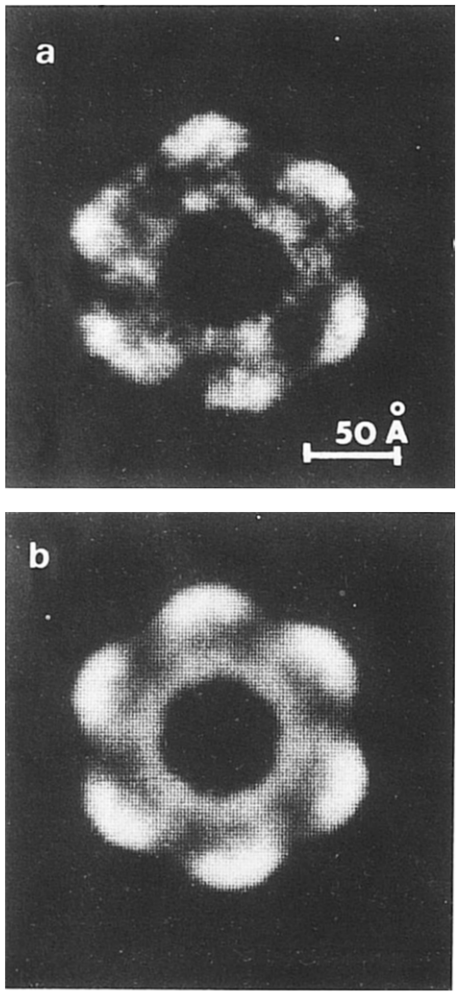


Fig. 6. Average of 15 particles with the highest correlation (a) before and (b) after sixfold rotational averaging.

## 5. Discussion

Except for the handedness of the stained molecule projection, which has not been previously observed, the shape of the molecule projection (fig. 7) agrees with that obtained by Valentine et al. for E coli GS. In our reconstruction however, the elliptic outside boundaries are slightly skewed, forming an angle of about 6° with the direction normal to the radius of the molecule.

The most pronounced feature in the stain-excluding region of the reconstruction is a low-density elliptic region at a radial distance of 61 Å, with the major axis skewed against the direction normal to the molecule radius by about 6°. The major and minor axes of the elliptical region are 42.5 and 24 Å long, respectively. These dimensions are based on Valentine et al.'s measurement of 140 Å for the outer diameter of the E. coli GS, since we expect the variation of the molecule size between species to be smal-

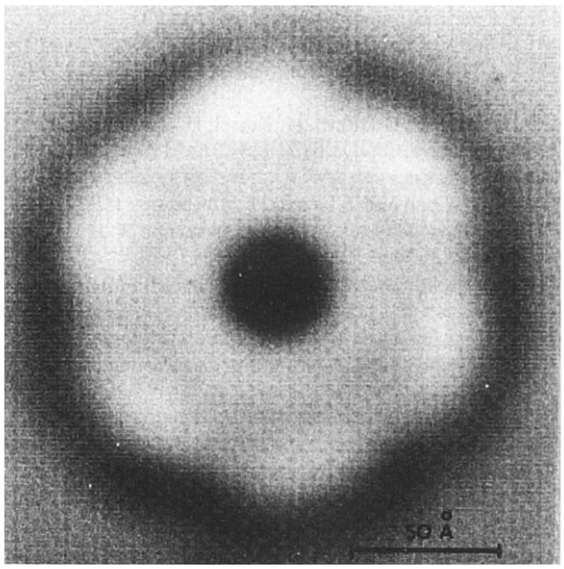


Fig. 7. Gray-level display of reconstructed particle, including highcontrast stain regions.

ler than the error of magnification calibration. With this scaling the magnification works out as 51 000X. The spiral arm and elliptic region form a roughly circular area with a diameter of 42.5 Å.

The most puzzling result is the evidence of handedness in the reconstructed projection. How can this finding be reconciled with the results of earlier studies which indicated dihedral point-group symmetry? We must assume that the stain distribution is consistently different on top of the particle (away from the carbon film) than on the bottom (the side attached to the carbon film). The contour map then contains some information on the structure of the single hexamer, but this is difficult to decipher without additional experiments using different stains and nonaxial projections of the particle.

Nonuniform stain distribution is well known in micrographs of virus particles. which are much larger than the GS molecules. Virus particles with a predominant sidedness in stain can often be picked out visually from others with more uniform staining on the same grid. When analyzed by optical diffraction, images of viruses and virus-related structures with helical symmetry give different sets of spots arising from the two sides of the particle [16]. This analysis can be used to verify the distinction between particles uniformly stained and those more strongly stained on one side.

Uniformity of stain distribution may also be strongly affected by the type of negative stain used. Nagington et al. [17] found that ammonium molybdate provided single-sided images of the spiral tubular thread structure in the wall of the Orf virus, while sodium phosphotungstic acid stain of the same virus showed discrete images of the top and bottom structures.

An alternative explanation may be a difference in shrinkage behavior between the top and bottom of the particle, if the bottom part is stabilized by the carbon film [18]. Because of the asymmetric structure of the subunits, which can be inferred from chemical data [3], such a shrinkage differential could distort the original dihedral point-group symmetry.

We have reconstructed GS particles from E. coli stained with ammonium molybdate, uranyl acetate, and phosphotungstic acid, as well as with uranyl formate. The results are very similar, with handedness evident in the reconstructions.

## 6. Conclusions

The full potential of the new computer averaging method will become available with the adoption of low-dose techniques and the replacement of stain by glass-like embedding media such as glucose. Preliminary averaging studies of subminimum-dose electron micrographs of stained GS [10,20] have confirmed the feasibility of the alignment procedure under these conditions.

The goal of the GS project is a high-resolution three-dimensional low-dose reconstruction of the molecule. Here the random azimuthal orientations of the particles will prove to be an advantage.

A single low-dose micrograph of a maximally tilted specimen will supply all the Fourier information contained in a cone up to that tilt angle. The missing part of the Fourier space can be recovered from a micrograph of long, stacked cylinders [4] (fig. 1).

Another application will be reconstruction from low-dose images of crystals with small patches of coherent order whose boundaries can be recognized in the high-dose reference image. Each such patch can be thought of as a particle and can be treated by the

same alignment and averaging procedures used in this investigation.

## Acknowledgements

We would like to thank Dr. F. Wedler, Rensselaer Polytechnic Institute, for a gift of glutamine-synthetase and Dr. M. Kessel of this Division for valuable discussions.

## References

[1] U. Aebi, P.R. Smith, J. Dubochet, C. Henry and E. Kellenberger, J. Supramol. Str. 1 (1973) 498.
[2] P.N.T. Unwin and R. Henderson, J. Mol. Biol. 94 (1975) 425.
[3] R.C. Valentine, B.M. Shapiro and E.R. Stadtmann, Biochemistry 7 (1968) 2143.
[4] T. Frey, D. Eisenberg and F.A. Eiserling, Proc. Nat. Acad. Sci. USA 72 (1975) 3402.
[5] W. Kabsch, H. Kabsch and D. Eisenberg, J. Mol. Biol. 100 (1976) 283.
[6] R. Markham, S. Frey and G.J. Hills, Virology 20 (1963) 88.
[7] J. Frank, Ultramicroscopy 1 (1975) 159.
[8] J. Frank, Ann. New York Acad. Sci. 306 (1978) 112.
[9] W.O. Saxton and J. Frank, Ultramicroscopy 2 (1977) 219.
[10] J. Frank, W. Goldfarb, M. Kessel, D. Eisenberg and T.S. Baker, Biophys. J. 21 (1978) 89a (Abstr).
[11] F.P. Ottensmeyer, J.W. Andrew, D.P. Bazett-Jones, A.S.K. Chan and J. Hewitt, J. Microscopy (1977) 259.
[12] R. Langer, J. Frank, A. Feltynowski and W. Hoppe, Ber. Bunsenges. Phys. Chem. 74 (1970) 1120.
[13] W.O. Saxton, Eighth Int. Congr. Electron Microscopy Canberra vol. I (1974) 314.
[14] J. Frank, in Advanced Techniques in Biological Electron Microscopy, ed. J. Koehler (Springer-Verlag, Berlin, 1973) p. 215.
[15] J. Frank and B. Shimkin, 9th Int. Cong. Electron Microscopy Toronto Vol. I (1978) p. 210.
[16] A. Klug and D. DeRosier, Nature 212 (1966) 29.
[17] J. Nagington, A.A. Newton and R.W. Horne, Virology 23 (1964) 461.
[18] M.F. Moody, Phil. Trans. Roy. Soc. Lond. B261 (1971) 181.
[19] J. Frank, The role of correlation techniques in computer image processing, in Computer Processing of Electron Microscope Images, ed., P.W. Hawkes (Springer-Verlag, Heidelberg, 1978) fig. 5.3, in press.
[20] J. Frank, W. Goldfarb and M. Kessel, 9th Int. Congr. Electron Microscopy, Toronto, Vol. II (1978) p. 8.